Nanomolar Detection of Glutamate at a Biosensor Based on Screen-Printed Electrodes Modified with Carbon Nanotubes

Raju Khan,[a, b] *Waldemar Gorski*,[b] *Carlos D. Garcia**[b]

[a] Analytical Chemistry Division, CSIR-North East Institute of Science & Technology, Jorhat, 785006, Assam, India
[b] Department of Chemistry, The University of Texas at San Antonio, One UTSA Circle, San Antonio, TX, 78249, USA
phone: 01 (210) 458-5774, fax: 01 (210) 458-5428
*e-mail: carlos.garcia@utsa.edu

Received: July 2, 2011
Accepted: August 15, 2011

Abstract
The flow injection analysis (FIA) of monosodium L-glutamate (MSG) was performed electrochemically using a biosensor based on screen-printed electrodes containing carbon nanotubes (CNT). The sensor was fabricated by simply adsorbing glutamate oxidase (GlutOx) on the electrode surface. The resulting device displayed excellent electroanalytical properties toward the determination of L-glutamate in a wide linear range (0.01–10 μM) with low detection limit (10 nM, $S/N \geq 3$), fast response time (≤ 5 s), and good operational and long-term stability. The CNT-modified screen-printed electrodes have a potential to be of general interest for easy preparation of electrochemical sensors and biosensors relevant for biomedical applications.

Keywords: Biosensors, L-Glutamate, Glutamate oxidase, Flow injection analysis, Carbon nanotubes

DOI: 10.1002/elan.201100348

1 Introduction

Biosensors have been applied in many fields including clinical diagnostics, food processing, and biomedical research in order to quantify the selected chemical species. Among others, the analysis of L-glutamate has received much attention recently. L-glutamate (Glut) is one of the most commonly found amino acids in nature [1] and has critical neurological functions including neurotransmission [2,3]. Monosodium L-glutamate (MSG) is also an important flavor enhancer, which is typically added to the processed meats, poultry, seafood, snacks, soups, and stews at a concentration ranging from 0.1 to 0.8 wt% [4]. Although most regulatory agencies have affirmed the safety of MSG, at levels normally consumed by the general population, many customers have the perception that glutamate may have detrimental health effects [4]. In response to such perception, and due to the important biological functions of L-glutamate, various instrumental methods based on liquid chromatography have been developed for its analysis [5,6]. Several alternative approaches have also been developed to quantify the L-glutamate including methods based on capillary electrophoresis [7], chemiluminometry [8], fluorescense [9], and electrochemistry. Although the electrochemical detection of L-glutamate is typically based on the use of enzymes immobilized in reactors [10], microdialysis probes [11], nanocomposites [12], or on gold surfaces [13], the most common detection technique is amperometry [14–18]. Some of the reasons for this trend include its simple instrumental setup, potential for miniaturization, sensitivity, and fast response.

Among other carbon-based materials, carbon nanotubes (CNT) are one of the preferred substrates for the design of biosensors [14,15]. Among other advantages it is worth highlighting high surface area [16] and the possibility to enhance the electrochemical reactivity of different biomolecules [14,17–20].

The present paper describes the amperometric biosensor for the flow injection analysis (FIA) at nM levels. The L-glutamate biosensor was prepared by adsorption of the enzyme L-glutamate oxidase (GlutOx) on a commercial screen-printed substrate containing CNT. In addition to providing a robust platform that integrates the working, counter, and reference electrodes, the selected substrate could be easily integrated in the FIA system, which facilitated sample-handling operations and improved the overall throughput of the analytical method. The following sections provide the characterization of the L-glutamate biosensor and the optimization of experimental conditions in order to maximize its signal. We also demonstrate the use of such sensor for the analysis of glutamate in a real sample (spiked soy sauce).

2 Experimental

2.1 Molecular Modeling

Molecular modeling calculations were performed in order to probe the interactions between the enzyme molecules

and carbon nanotubes. The docking of a GlutOx molecule to a 5-nm long single-wall carbon nanotube (Nanotube Modeler V 1.7.1, JCrystalSoft) was modeled using AutoDock Vina 4.2 [21] and the X-ray crystal structure of the enzyme (PDB ID: 2E1 M) [22]. The grid box with dimensions of 100 Å in the *X*, *Y*, and *Z* directions was used with its center placed at the center of the enzyme molecule. This grid size was selected in order to include the entire enzyme molecule and, thus, allowing the CNT to randomly interact with the whole surface of the protein. The spacing was set at 0.653 Å, which defined 1,030,301 points for analysis. The calculations did not include the solvent effects or post-adsorption structural rearrangements of the enzyme. Out of the nine potential docking sites identified by the model, the preferred configuration was defined as the one with the minimum potential energy and maximum number of poses clustered at that site. The calculations lasted less than 5 h when performed on a MacBook Air (2.13 GHz Intel core duo processor, 4GB RAM memory, and Leopard 10.6.7). The graphical analysis of the results was performed by using the PyMol molecular visualization program [23].

2.2 Regents and Solutions

The aqueous solutions were prepared by using analytical grade regents and ultrapure water (18 MΩ cm^{-1}, NANOpure Diamond; Barnstead, Dubuque, IA). L-glutamate oxidase (from *Streptomyces* sp., $\geq$5.0 U.mg^{-1}), H_2O_2, sodium L-glutamate, L-cysteine, acetaminophen, and L-ascorbic acid were purchased from Sigma–Aldrich (Saint Lois, MO). Other chemicals ($NaH_2PO_4{\cdot}H_2O$, Na_2HPO_4, HCl, and NaOH) were purchased from Fisher Scientific (Fairlawn, NJ). Sodium phosphate buffer solution (0.10 M, pH 7.40) was prepared daily and used as a background electrolyte for the electrochemical detection as well as a carrier solution in the flow injection system. Stock solutions of glutamate (0.100 M) were prepared in phosphate buffer solutions. All experiments were performed at room temperature (22 $\pm$ 1 °C).

2.3 Electrochemical Measurements

A CHI-810B workstation (CH Instruments; Austin, TX) was used to characterize the biosensors and to perform the electrochemical detection experiments. In all cases, the commercial screen-printed electrode substrates (DRP-110CNT, DropSens; Asturias, Spain) with 4.0-mm dia. multiwall CNT-COOH working electrode, carbon ink counter electrode, and an integrated silver pseudo-reference electrode were used. The pseudo-reference electrode had a potential of +20 mV vs. conventional Ag/AgCl/NaCl 3 M reference electrode when measured in 0.10 M phosphate buffer (pH 7.40).

2.4 Biosensor Preparation

In order to prepare the biosensors, 10.0 μL of a freshly prepared solution of L-glutamate oxidase ($\geq$5.0 U mL^{-1}) was cast on the working electrode and incubated at 4 °C overnight. The conditions for the immobilization of the enzyme were selected based on prior studies from our group [24–27]. The biosensors were rinsed with a buffer solution to remove loosely-bound material and stored at 4 °C in pH 7.40 phosphate buffer solution when not in use.

2.5 Flow Injection Analysis

The FIA experiments were carried out by using a homemade flow system that comprised a 12-cylinder peristaltic pump (Gilson Minipuls 3; Middleton, WI), manual six-port rotary injection valve (Rheodyne 9725; Rohnert Park, CA), and wall-jet flow cell (DropSens; Asturias, Spain) placed downstream. The injection valve included a 20-μL sample loop (PEEK tubing, 0.020" *ID* × 1/16" *OD* × 10.1 cm, Upchurch Scientific; Oak Harbor, WA). The DropSens wall-jet cell for FIA was composed of two transparent methacrylate blocks with the inlet and outlet flow channels that impinged the carrier solution on the detection electrode. The open-close system (no screws needed) of the flow cell allowed for easy sensor replacement. After the modification of the working electrode with the enzyme solution, the screen-printed electrode substrate was placed in between the cell blocks and connected to the potentiostat using an ad-hoc connector. The system was flushed with the carrier solution to remove the bubbles and the baseline current was recorded. Once the baseline was stabilized (<5 min), the solutions containing the selected analyte (L-glutamate or hydrogen peroxide) were injected into the flow stream and the FIAgram was recorded at a selected constant potential. The data points and error bars presented in this manuscript represent the average peak currents and standard deviations, respectively, of at least three consecutive injections.

3 Results and Discussion

3.1 Molecular Modeling Studies

The AutoDock Vina molecular docking program was used to identify the most likely mode by which the enzyme molecule adsorbs to a single carbon nanotube. Figure 1 shows that the identified docking site involved the interactions of CNT with random coil structures of the enzyme. The overall calculated binding energy was equal to −28.0 kcal mol^{-1}, which indicated that the adsorption was sufficient to immobilize the GlutOx on the surface of CNT. In addition, the molecular visualization indicated that the adsorption of enzyme molecules on carbon nanotubes should not affect the accessibility of the active sites (Argyr124, Arg305, His312, Gly316,

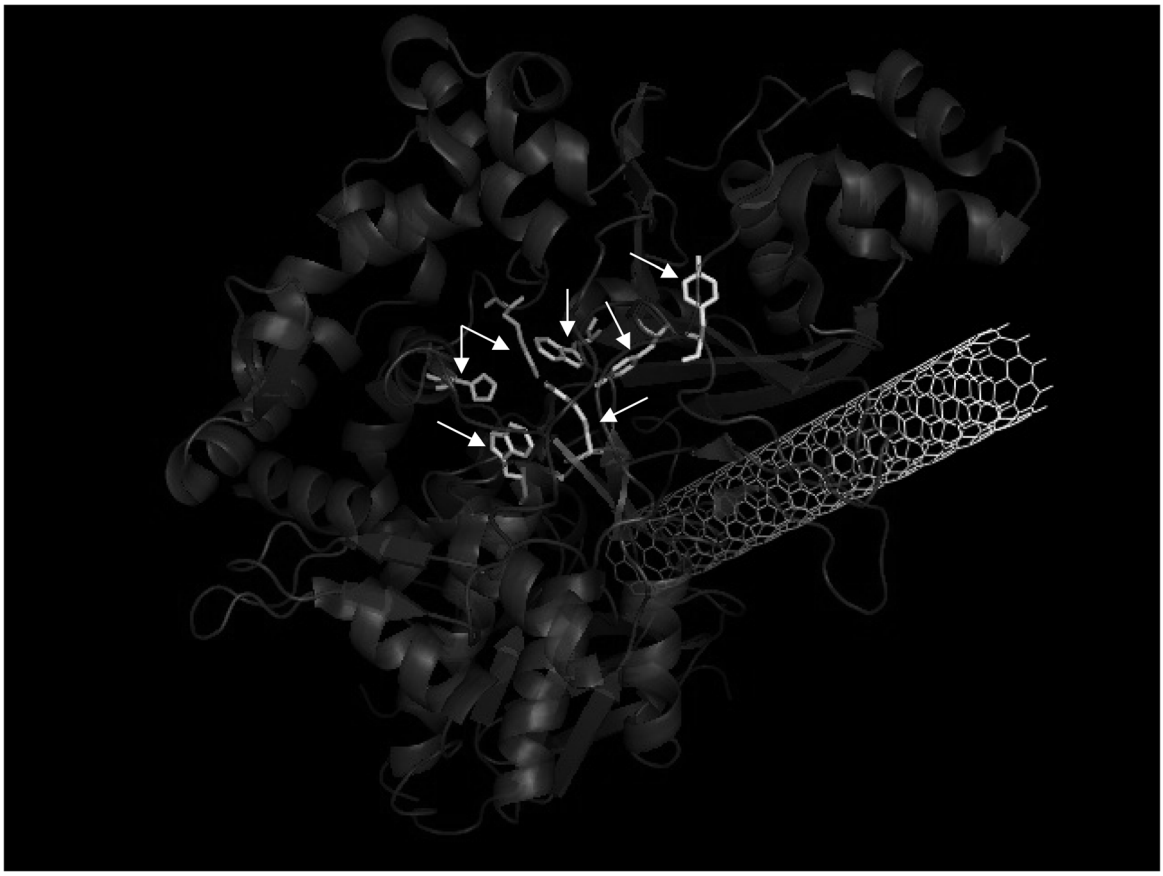

Fig. 1. Binding pose of GlutOx on the CNT according to the AutoDock Vina molecular docking program. The amino acids of the enzyme's active site are indicated by arrows.

Tyr545, Tyr562, Trp564, and Trp653) [22] to L-glutamate molecules.

3.2 Substrate Characterization

The surface of the working electrodes on the substrates was investigated by scanning electron microscopy (SEM). Figure 2 shows that the working electrode was made of a highly porous matrix with embedded CNT. Such CNT-based matrices have shown good capacity for enzyme immobilization [28,29] and electrooxidation of hydrogen peroxide produced by enzymatic reactions [30]. The extended network of nanopores results in the increased roughness of the electrode surface, which leads to the increased active surface area and better sensitivity of such devices [16]. These features in conjunction with the low cost and robustness of such electrodes are very attractive in the development of sensitive biosensors.

The voltammetric properties of the plain electrodes were investigated by recording cyclic voltammograms in a pH 7.40 phosphate buffer solution (data not shown). The voltammograms were featureless in a wide potential window (from −0.5 to 1.2 V vs. the Ag pseudo-reference electrode) and revealed relatively low background currents ($<0.6\ \mu A$).

3.3 Selection of Detection Potential

The H_2O_2 produced in the enzymatic reactions of oxidases can be detected electrochemically under a variety of conditions [31,32]. One of the key parameters in the operation of electrochemical biosensors is the potential applied to a working electrode. Higher detection potentials typically yield higher signals (peak currents) but they typically result in poorer selectivity and longer baseline stabilization time. In order to determine the optimum detection potential, a hydrodynamic voltammogram was obtained by performing sequential injections of 10.0-μM glutamate aliquots into a flowing solution and changing the applied potential in the 0.60–1.20 V range. Figure 3 summarizes the relationship between the analyte peak current and the potential applied to the working electrode for both the L-glutamate and hydrogen peroxide.

Figure 3 shows that the biosensor did not respond to the injection of either L-glutamate or H_2O_2 at potentials lower than 0.7 V. At higher potentials, the parallel increase in the peak current for both the L-glutamate and H_2O_2 was observed. Such behavior supports the notion that the glutamate detection was via the oxidation of H_2O_2 that was produced in the enzymatic Reaction 1.

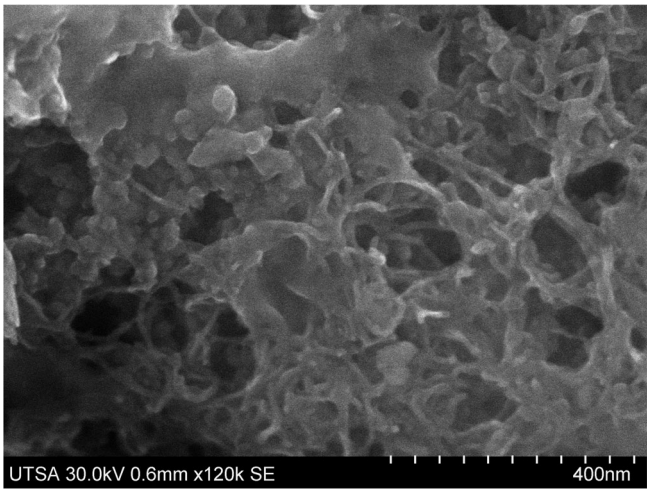

Fig. 2. SEM micrograph of the surface of screen printed electrodes containing multiwall CNT.

$$\text{L-glutamate} + O_2 + H_2O_2 \xrightarrow{\text{GlutOx}} \text{L-ketoglutarate} + H_2O_2 + NH_3 \quad (1)$$

In order to preserve practical sensitivity and avoid longer baseline stabilization times at high positive potentials, a detection potential of 0.95 V was selected and used for the rest of the experiments described in this manuscript. Although the oxidation of hydrogen peroxide at 0.95 V proved to be a simple working approach to the signal transduction in the proposed biosensor (vide infra), the use of high detection potentials can limit the selectivity of the sensor. In such cases, the alternative option would be to use the low-potential reduction of hydrogen peroxide catalyzed by horseradish peroxidase [33]. However, that alternative would require the incorporation of a second enzyme into the biosensor [34,35].

The stability of the signal at 0.95 V was examined by performing consecutive injections of 10.0 μM H_2O_2 (data not shown). Only negligible changes in peak current were observed, which indicated the relevance of screen-printed electrodes as suitable substrates for the development of electrochemical biosensors.

3.4 Selection of Flow Rate

The effect of flow rate on the response of the biosensor was studied by injecting 10.0-μM aliquots of L-glutamate in the flow injection analysis system.

Figure 4 shows that the peak current due to the L-glutamate injection was higher at lower flow rates. This can be explained by considering that at low flow rates the residence time of L-glutamate in the detection cell is longer, which allows for the generation of more hydrogen peroxide (as shown in Reaction 1). This, in turn, leads to larger peak current due to the electro-oxidation of hydrogen peroxide. However, the application of very low flow rates negatively affected the widths of the injection peaks (e.g. they increased from 9 ± 1 s at 6.0 mL min^{-1} to 35 ± 1 s at 1 mL min^{-1}), which ultimately determine the throughput of the analytical technique. In order to preserve a good signal-to-noise ratio along with the acceptable sampling frequency (up to 7 samples min^{-1}), the flow rate of 3.0 mL min^{-1} was selected as optimal and used in all subsequent experiments.

3.5 Selection of pH

The effect of pH on the peak current was investigated in the pH range from 6.6 to 8.0 by injecting 10.0-μM aliquots of glutamate solution into the carrier solution. Outside of

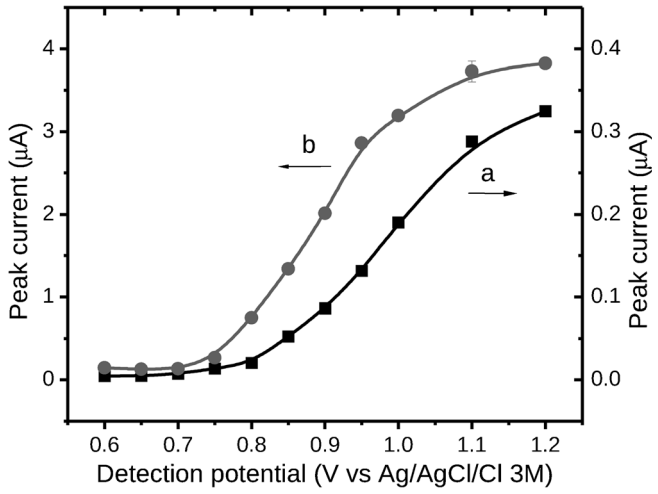

Fig. 3. Hydrodynamic voltammograms of (a) 10 μM L-Glutamate, and (b) 10 μM H_2O_2 recorded at the biosensor. Carrier solution, pH 7.40 phosphate buffer (0.10 M). Flow rate, 3.0 mL min^{-1}.

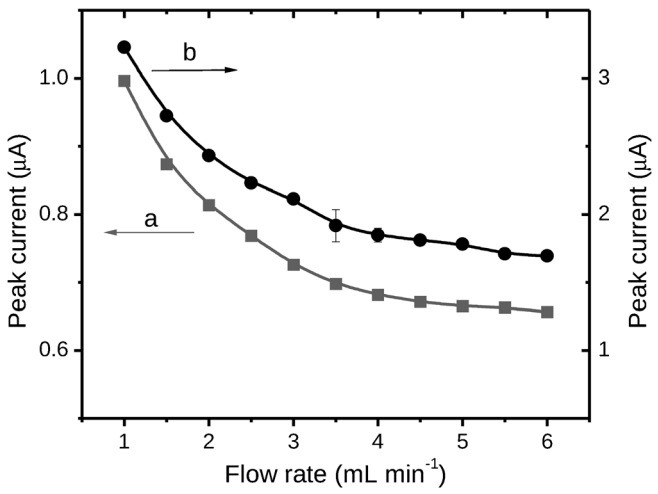

Fig. 4. The effect of flow rate on the current response of the biosensor to (a) 10.0 μM L-glutamate, and (b) 10 μM H_2O_2. Carrier solution, pH 7.40 phosphate buffer (0.10 M). Potential, 0.95 V.

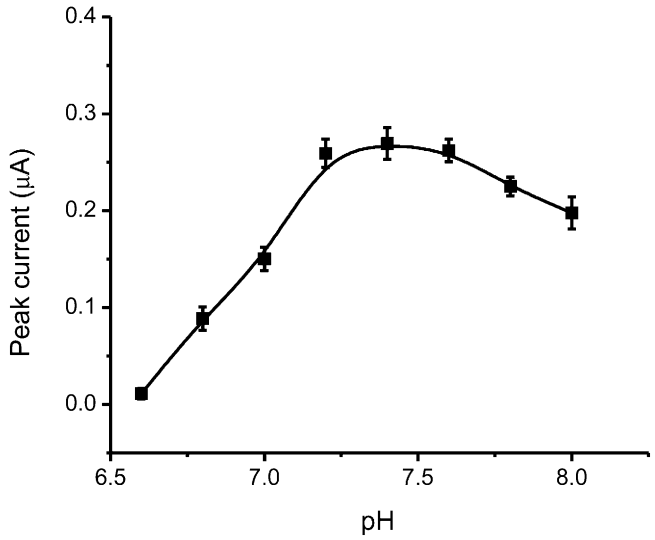

Fig. 5. Effect of pH on the amperometric response of the biosensor to 10.0 μM L-glutamate. Carrier solution, pH 7.40 phosphate buffer (0.10 M). Flow rate, 3.0 mL min^{-1}. Potential, 0.95 V.

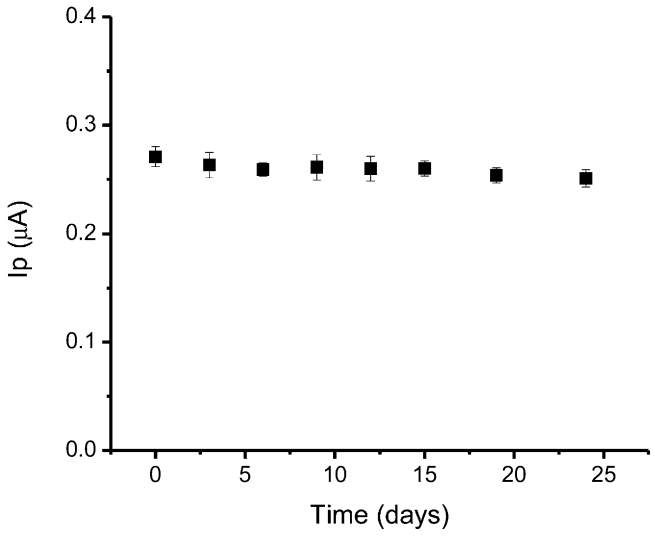

Fig. 6. Shelf-stability of the biosensor measured by sequential injections of 10.0 μM L-glutamate solution into a carrier solution. Carrier solution, pH 7.40 phosphate buffer (0.10 M). Flow rate, 3.0 mL min^{-1}. Potential, 0.95 V.

this pH range, a significant enzyme denaturing was observed in accordance with the previous reports [36].

Figure 5 shows a bell-shaped current – pH curve with a maximum response in the pH range from 7.2 to 7.6. This range includes the optimum pH 7.4, which was reported for the free GlutOx enzyme [36]. This suggests that the enzymatic reaction rather than the electrochemical oxidation of H_2O_2 determines the response of the biosensor to L-glutamate. In order to maximize the biosensor's signal, a phosphate buffer solution (pH 7.4) was selected as the optimum carrier solution for all further experiments.

3.6 Analytical Figures of Merit

Under the optimized experimental conditions, the linear relationship between the L-glutamate concentration and the biosensor's signal extended over the three orders of magnitude (0.01–10 μM). The sensitivity of the detection, as defined by the slope of the linear range of the calibration curve, was equal to 0.72 ± 0.05 μA μM^{-1} ($R = 0.970$). The reproducibility of the signal was evaluated by recording the peak current due to the injection of 10.0 μM L-glutamate solution into the FIA system. The relative standard deviation of the average peak current was below 6% ($N = 50$). In order to examine the long-term storage stability, the response of the biosensor was examined by performing 20 consecutive injections of 10.0 μM L-glutamate aliquots every 3 days during a 24-day test period. The biosensor was rinsed with a buffer solution and stored in a pH 7.40 phosphate buffer solution at 4 °C when not in use. Figure 6 shows that the biosensor retained 92% of its initial signal after 24 days. This documents a good long-term stability of the glutamate oxidase in the proposed biosensor. This also corroborates prior reports stating that the adsorption of enzymes on the CNT is predominantly irreversible [2, 16, 24–26] and that some of the enzyme adsorbed on the CNT can undergo deactivation.

The biosensor's response to some of the most common potential interferences (ascorbic acid, L-cysteine, and acetaminophen) was also investigated. Figure 7 shows that at a concentration level of 100 μM (10 times higher than that of L-glutamate) the interference level of the three species was approximately 3%. It should be pointed out that we recorded a high level of interference from L-cysteine and acetaminophen but at alkaline pH values (pH > 10, data not shown), which is in agreement with previous reports [28].

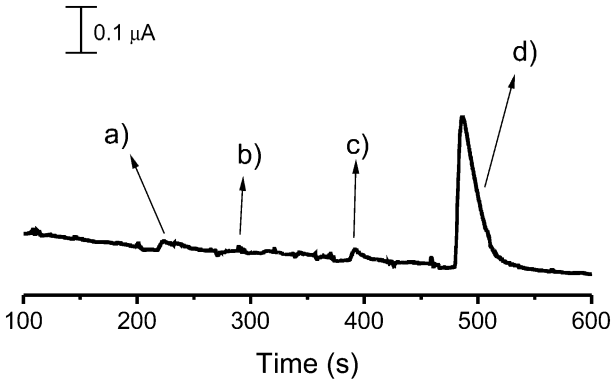

Fig. 7. Amperometric trace recorded at the biosensor for injections of (a) 100 μM ascorbic acid, (b) 100 μM L-cysteine, (c) 100 μM acetaminophen, and (d) 10 μM L-glutamate. Carrier solution, pH 7.40 phosphate buffer (0.10 M). Flow rate, 3.0 mL min^{-1}. Potential, 0.95 V.

Table 1. Comparison of selected electrochemical biosensors for L-glutamate.

Electrode	E_{DET} (V)	Linear range (μM)	Response time (s)	Ref.
SPE	0.95 [a]	0.01–10	5	This work
CNT/Chitosan	0.40 [b]	0.5–200	2	[37]
CNT/Chitosan	0.40 [b]	0.5–500	2	[38]
(Pt-PAMAM)nCNTs	0.20 [b]	0.2–250	3	[17]
Pt-DENs/CNTs/Ppy	0.20 [b]	0.1–60	3	[18]
PPy/MWCNT	1.10 [b]	0.3–140	7	[39]
Th-MWCNTs	0.145 [b]	0.1–500	3	[40]
Th-SWNTs	0.19 [b]	0.5–400	5	[41]
CSCNTsGC	0.0 [b]	0.003–10	–	[42]

[a] vs. integrated pseudo-reference electrode; [b] vs. Ag/AgCl/3 M NaCl reference electrode, SPE: screen printed electrode, PAMAM: Poly(amido amine), DENs: dendrimers, Ppy: Polypyrrole; MWCNT: multiwall carbon nanotubes, SWCNT: single-wall carbon nanotubes, CSCNT: cup-stacked carbon nanotubes, GC: glassy carbon.

3.7 Determination of L-Glutamate in Real Samples

The biosensor was used to determine the L-glutamate in a real sample of soy sauce. The sample, that contained no MSG, was spiked to a final concentration of 10 μM L-glutamate and analyzed by the standard addition method using the optimized conditions. This method was selected because of the presence of other electrochemically-active compounds in the as-received sample. The analysis yielded a concentration of 9.8 ± 0.1 μM ($N = 3$), which illustrated the merit of the proposed biosensor for the determination of L-glutamate in the matrix of soy sauce.

3.8 Comparison with Other Electrochemical L-Glutamate Biosensors

Table 1 shows a comparison of our biosensor with other relevant glutamate biosensors published in open literature. The proposed new biosensor displays a wide linear range of three orders of magnitude, which is comparable to that of the other biosensors. However, it displays a very low detection limit (10 nM), which is among the best reported thus far. Other advantageous features of the proposed biosensor include the use of a commercially-available electrode substrate combined with the simplicity of enzyme immobilization.

4 Conclusions

The results described in this paper demonstrate the feasibility of fabricating biosensors by simply adsorbing enzymes on a commercially-available screen-printed substrate modified with carbon nanotubes. Such approach allows for the development of reliable sensors with detection limits in the nanomolar range. The integration of such biosensors with flow injection analysis systems facilitates the sampling and handling operations, therefore improving the throughput of the method.

Acknowledgements

Financial support for this project was provided by the *Welch Foundation Departmental Research* Grant (AX-0026), National Institutes of Health through the National Institute of General Medical Sciences (1SC3GM081085), and the *Research Centers at Minority Institutions* (2G12RR013646-11). Dr. R. Khan is thankful to the *Department of Science & Technology (DST), Government of India* for financial support received under the BOYSCAST Fellowship No. SR/BY/C-09/09. Authors would also like to thank Dr. Murilo Cabral (University of Sao Paulo) for useful discussions and help with the AutoDock program.

References

[1] S. Jinap, P. Hajeb, *Appetite* **2010**, *55*, 1.
[2] T. P. Obrenovitch, *Ann. NY Acad. Sci.* **1999**, *890*, 273.
[3] E. Naylor, D. V. Aillon, S. Gabbert, H. Harmon, D. A. Johnson, G. S. Wilson, P. A. Petillo, *J. Electroanal. Chem.* **2011**, *656*, 106.
[4] J. Prescott, A. Young, *Appetite* **2002**, *39*, 25.
[5] G. Halmos, B. Lendvai, A. Gáborján, M. Baranyi, L. Z. Szabó, L. Csokonai Vitéz, *Neurochem. Int.* **2002**, *40*, 243.
[6] V. P. Hanko, J. S. Rohrer, *Anal. Biochem.* **2004**, *324*, 29.
[7] L. A. Dawson, J. M. Stow, A. M. Palmer, *J. Chromatogr. B* **1997**, *694*, 455.
[8] N. Kiba, T. Miwa, M. Tachibana, K. Tani, H. Koizumi, *Anal. Chem.* **2002**, *74*, 1269.
[9] R.-A. Doong, H.-M. Shih, *Biosens. Bioelectron.* **2006**, *22*, 185.
[10] K. Hayashi, R. Kurita, T. Horiuchi, O. Niwa, *Biosens. Bioelectron.* **2003**, *18*, 1249.
[11] A. Morales-Villagrán, C. Sandoval-Salazar, L. Medina-Ceja, *Neurochem. Res.* **2008**, *33*, 1592.
[12] S. Chakraborty, C. Retna Raj, *Electrochem. Commun.* **2007**, *9*, 1323.
[13] L. Muresan, M. Nistor, S. Gáspár, I. C. Popescu, E. Csöregi, *Bioelectrochemistry* **2009**, *76*, 81.
[14] M. Wooten, W. Gorski, *Anal. Chem.* **2010**, *82*, 1299.
[15] K. Scida, P. W. Stege, G. Haby, G. A. Messina, C. D. Garcia, *Anal. Chim. Acta* **2011**, *691*, 6.
[16] M. R. Nejadnik, L. Francis, C. D. Garcia, *Electroanalysis* **2011**, *23*, 1462.

[17] L. Tang, Y. Zhu, L. Xu, X. Yang, C. Li, *Talanta* **2007**, *73*, 438.
[18] L. Tang, Y. Zhu, X. Yang, C. Li, *Anal. Chim. Acta* **2007**, *597*, 145.
[19] M. Zhang, W. Gorski, *Anal. Chem.* **2005**, *77*, 3960.
[20] M. Zhang, A. Smith, W. Gorski, *Anal. Chem.* **2004**, *76*, 5045.
[21] O. Trott, A. J. Olson, *J. Comp. Chem.* **2010**, *31*, 455.
[22] J. Arima, C. Sasaki, C. Sakaguchi, H. Mizuno, T. Tamura, A. Kashima, H. Kusakabe, S. Sugio, K. Inagaki, *FEBS J.* **2009**, *276*, 3894.
[23] T*he {PyMOL} Molecular Graphics System*, Version 1.3, Schrödinger LLC **2010**.
[24] J. L. Felhofer, J. Caranto, C. D. Garcia, *Langmuir* **2010**, *26*, 17178.
[25] M. F. Mora, C. E. Giacomelli, C. D. Garcia, *Anal. Chem.* **2009**, *81*, 1016.
[26] L. E. Valenti, P. A. Fiorito, C. D. Garcia, C. E. Giacomelli, *J. Colloid Interf. Sci.* **2007**, *307*, 349.
[27] J. Wehmeyer, R. Bizios, C. D. Garcia, *Mat. Sci. Eng. C* **2010**, *30*, 277.
[28] P. Fanjul-Bolado, D. Hernández-Santos, P. J. Lamas-Ardisana, A. Martín-Pernía, A. Costa-García, *Electrochim. Acta* **2008**, *53*, 3635.
[29] R. O. Kadara, N. Jenkinson, C. E. Banks, *Sens. Actuators B* **2009**, *138*, 556.
[30] P. Fanjul-Bolado, P. Queipo, P. J. Lamas-Ardisana, A. Costa-García, *Talanta* **2007**, *74*, 427.
[31] L. Blanes, M. F. Mora, C. L. do Lago, A. Ayon, C. D. Garcia, *Electroanalysis* **2007**, *19*, 2451.
[32] M. R. Nejadnik, C. D. Garcia, *Colloids Surf. B* **2011**, *82*, 253.
[33] A. A. Karyakin, O. V. Gitelmacher, E. E. Karyakina, *Anal. Chem.* **1995**, *67*, 2419.
[34] A. Salimi, R. G. Compton, R. Hallaj, *Anal. Biochem.* **2004**, *333*, 49.
[35] P. Santhosh, K. M. Manesh, K.-P. Lee, A. I. Gopalan, *Electroanalysis* **2006**, *18*, 894.
[36] M. Sukhacheva, A. Netrusov, *Microbiology* **2000**, *69*, 17.
[37] M. Zhang, C. Mullens, W. Gorski, *Electrochim. Acta* **2006**, *51*, 4528.
[38] M. Zhang, C. Mullens, W. Gorski, *Electroanalysis* **2005**, *17*, 2114.
[39] M. Ammam, J. Fransaer, *Biosens. Bioelectron.* **2010**, *25*, 1597.
[40] M. M. Rahman, A. Umar, K. Sawada, *J. Phys. Chem. B* **2009**, *113*, 1511.
[41] L. Meng, P. Wu, G. Chen, C. Cai, Y. Sun, Z. Yuan, *Biosens. Bioelectron.* **2009**, *24*, 1751.
[42] T. Noda, T. Ukai, T. Yao, *Anal. Sci.* **2010**, *26*, 675.

